Strategies for Sperm Chemotaxis in the Siphonophores and Ascidians: A Numerical Simulation Study

MAKIKO ISHIKAWA[1,*], HIDEKAZU TSUTSUI[1,†], JACKY COSSON[2], YOSHITAKA OKA[1,‡],
AND MASAAKI MORISAWA[1]

[1] *Misaki Marine Biological Station, Graduate School of Science, The University of Tokyo, Japan; and*
[2] *Observatoire Oceanologique de Villefrance-sur-Mer, CNRS, France*

Abstract. Chemotactic swimming behaviors of spermatozoa toward an egg have been reported in various species. The strategies underlying these behaviors, however, are poorly understood. We focused on two types of chemotaxis, one in the siphonophores and the second in the ascidians, and then proposed two models based on experimental data. Both models assumed that the radius of the path curvature of a swimming spermatozoon depends on $[Ca^{2+}]_i$, the intracellular calcium concentration. The chemotaxis in the siphonophores could be simulated in a model that assumes that $[Ca^{2+}]_i$ depends on the local concentration of the attractant in the vicinity of the spermatozoon and that a substantial time period is required for the clearance of transient high $[Ca^{2+}]_i$. In the case of ascidians, trajectories similar to those in experiments could be adequately simulated by a variant of this model that assumes that $[Ca^{2+}]_i$ depends on the time derivative of the attractant concentration. The properties of these strategies and future problems are discussed in relation to these models.

Introduction

After the first discovery of the chemotactic behavior of spermatozoa toward an egg by Dan (1950), sperm chemotaxis has been reported in various animal species (Miller, 1977; Eisenbach, 1999), and chemoattractants that mediate such behaviors have been identified in a few cases (Ward *et*

al., 1985; Coll *et al.,* 1994; Olson *et al.,* 2001; Yoshida *et al.,* 2002). Furthermore, recent cell biological studies revealed some of the intracellular enzymatic signaling cascade evoked by the attractant stimulations (Yoshida *et al.,* 2003; Kaupp *et al.,* 2003). However, a major question that anyone who observed this phenomenon has to bear in mind remains poorly answered: How does such a tiny spermatozoon succeed in finding an attractant source?

What makes this question both more mysterious and more interesting is the fact that distinct swimming trajectories have been observed for spermatozoa of different species, which implies that different strategies for chemotaxis may underlie these behaviors. For example, the chemotactic behavior in the siphonophores has been described as follows (Cosson *et al.,* 1984): spermatozoa show trajectories of large diameter (700–1000 μm) while swimming far from the "cupule," which in these species is an extracellular structure of the egg and serves as an attractant source, and trajectories of smaller diameter (200 μm) in the vicinity of the cupule; the transition between the two modes is progressive. In the ascidians, on the other hand, spermatozoa exhibit characteristic "chemotactic turns" during chemotaxis, but the curvature of the trajectories has no noticeable dependence on the distance to the attractant source (Yoshida *et al.,* 1993, 2002; Ishikawa, 2000). The behavior of sea urchin spermatozoa seems to be a little more complicated but still exhibits unambiguous chemotaxis (Ward *et al.,* 1985). Thus, it appears that spermatozoa in different species often respond to the attractant differently, although the goal is the same in all cases—to find an egg and facilitate fertilization.

One approach to revealing the underlying strategies for sperm chemotaxis may be to build a model based on the experimental observations and then study how the model works. In the present paper, we propose two models, one

applied to the siphonophores and the second to the ascidians. We focused on these two taxa because their swimming behaviors are simple but clearly distinct, and also because substantial experimental data are available in the literature (see Results for details). These experimental results were simplified, as summarized in Figure 1, and incorporated into the models, which required only a few simple and reasonable assumptions. We show that numerical calculations of sperm trajectory using the two models result in trajectories very similar to those observed experimentally.

Materials and Methods

General remarks on the models

It has been suggested that spermatozoa swim with three-dimensional beating waves whose characteristics confine them to a two-dimensional space when they are confronted with the interfaces between two media such as water/air or glass/water (Cosson *et al.*, 2003). For this reason as well as to simplify the observation of sperm trajectories under a microscope, our experiments have been restricted mainly to

spermatozoa located at the glass/water interface of the laboratory chambers. Since experimental background is necessary to test the validity of a model, the models we used were also limited to two dimensions. At the interface, most spermatozoa of siphonophores and ascidians show circular movement, usually in one preferred direction. A reasonable explanation is that the movement in the three-dimensional free environment is helical and that some of the initially homogeneously suspended spermatozoa were going upward and tended to be confined to the air/water interface, while others were going downward, to the water/glass interface, as was shown for sea urchin spermatozoa (see Cosson *et al.*, 2003). Sperm confined to the glass surface still exhibit unambiguous chemotaxis as reported thus far, and this behavior is our topic in the present study.

In our model, a spermatozoon is treated as a mathematical point. This point circulates in the x-y plane in one direction (clockwise for the ascidian spermatozoa observed in the vicinity of the glass slide surface, and counterclockwise for the siphonophore spermatozoa), with a radius of curvature that changes depending on the attractant concentration and
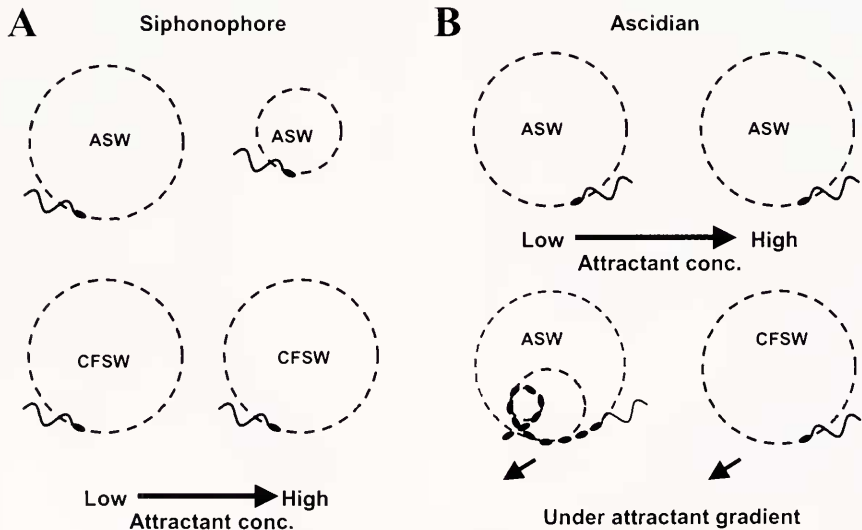

Figure 1. A summary, based on previous reports, of spermatozoa behavior in the presence of the attractant in two species of siphonophore (*Muggiaea kochi, Chelophyes appendiculata*) and one species of ascidian (*Ciona intestinalis*). (A) In the siphonophores, the curvature is negatively dependent on the attractant concentration in artificial seawater (ASW, *top*), but the dependence is lost in Ca^{2+}-free seawater (CFSW, *bottom*). (B) In the ascidians, no such dependence is observed, even in ASW (*top*), but a rapid modulation of the curvature leading to a turning behavior occurs in the presence of the attractant gradient (*bottom left*). Arrows indicate direction of the attractant source. The curvature is larger when swimming toward the source and smaller when swimming in the opposite direction. A short delay in the response has been often observed in this correlation (Ishikawa, 2000; Yoshida *et al.*, 2002). In CFSW, no such modulation in the curvature is observed, even under the attractant gradient (*bottom left*).

on time. Let us define some parameters: t, time; $p(t)$, position of sperm at t; $r(t) = v\{\cos(\phi(t)), \sin(\phi(t))\}$, velocity vector of sperm; $r(t)$, curvature; and $c(p)$, attractant concentration sensed by the sperm at position p (Fig. 2A). Since no significant changes in the swimming velocity were found during the chemotactic behavior in these species (Cosson *et al.*, 1984; Ishikawa, 2000; Yoshida *et al.*, 2002), let us assume the amplitude of the velocity vector as constant ($=v$). Numerical integration of sperm movement was evaluated as follows with a time step (Δt) of 1.0 ms:

$$p(t + \Delta t) = p(t) + \Delta t v(t) \qquad \text{(Eq. 1)}$$

$$\phi(t + \Delta t) = \phi(t) + \Delta t v/r(t) \qquad \text{(Eq. 2)}$$

Updating the angular component of velocity, but not the vector itself, as in the equation (2), moderates the accumu-
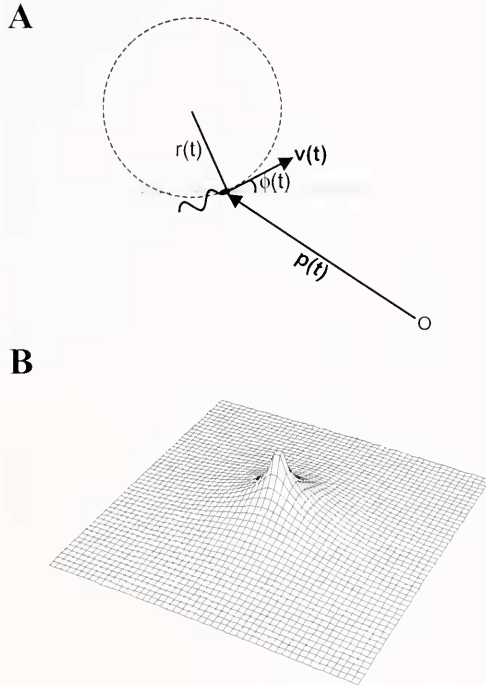
A

B

Figure 2. (A) A schematic drawing that shows the four parameters used in the calculation of sperm trajectory. O, the origin; p, position at t (vector); v, velocity (vector); ϕ, angular component of v (scalar); r, radius of curvature (scalar). (B) A computed snapshot of the chemoattractant gradient used in the present study. The attractant concentration profile in the square area of ± 1 mm of the x-y plane is plotted in the z-axis. The peak (hilltop) corresponds to the chemoattractant source located at the origin ($x = y = 0$).

lation of error during the integrations for a long time period. All the calculations and graphical outputs were done by using the Mathematica 3.0 program (Wolfram Research).

Attractant profile

For most observations of chemotaxis, the following experimental design was adopted: a glass pipette filled with chemoattractant or any fluid (within agar-gel in many cases) to be tested was placed in a drop of water containing dispersed sperm cells. This allows a spatial gradient of attractant concentration to be established rapidly: sperm located in the vicinity of an attractant source usually approach it within no more than tens of seconds. Since molecules such as an organic compound or a small protein normally have diffusion coefficients in water of $\sim 10^{-10}$ m^2/s or smaller, it is an acceptable approximation that the attractant profile does not change much during the approach of the spermatozoon. In our model, therefore, we simply used a computed snapshot of a solution of a diffusion equation as an attractant profile (Fig. 2B). Moreover, the drop is largely spread on the slide but is much thinner in the z-axis, so variation of attractant concentration along the z-axis should be small. Therefore, we consider the attractant gradient field with a two-dimensional diffusion equation with a coefficient of D:

$$\delta c/\delta t = D(\delta^2 c/\delta x^2 + \delta^2 c/\delta y^2) \qquad \text{(Eq. 3)}$$

In the polar coordinates of ρ, θ ($x = \rho \cos(\theta)$, $y = \rho \sin(\theta)$), equation (3) can be expressed as

$$\delta c/\delta t = D(\delta^2 c/\delta \rho^2 + 1/\rho \delta c/\delta \rho + 1/\rho^2 \delta^2 c/\delta \theta^2) \qquad \text{(Eq. 4)}$$

Since we assume a situation of spatial symmetry, the last term of equation (4) can be regarded to be zero,

$$\delta c/\delta t = D(\delta^2 c/\delta \rho^2 + 1/\rho \delta c/\delta \rho) \qquad \text{(Eq. 5)}$$

As a boundary condition, we assumed that the concentration at the origin (*i.e.*, the tip of a pipette) is always kept at a high level ($c(0) = 1$). We set D as 2.0×10^{-10} m^2/s and used a numerical solution of equation (5) at $t = 60$ s as the profile for subsequent trajectory calculations (Fig. 2B). We also tried some other static attractant profile models (exponential, parabolic, solution of the diffusion equation at different times, etc.) and found that most definitions resulted in qualitatively similar responses to what we show next.

Results

The siphonophore model

Some properties of sperm-swimming in siphonophores are summarized in Figure 1A. This summary is based on observations of *Muggiaea kochi* and *Chelopheyes appendiculata* (Cosson *et al.*, 1984). In artificial seawater (ASW), the spermatozoa show trajectories of larger diameter (700–
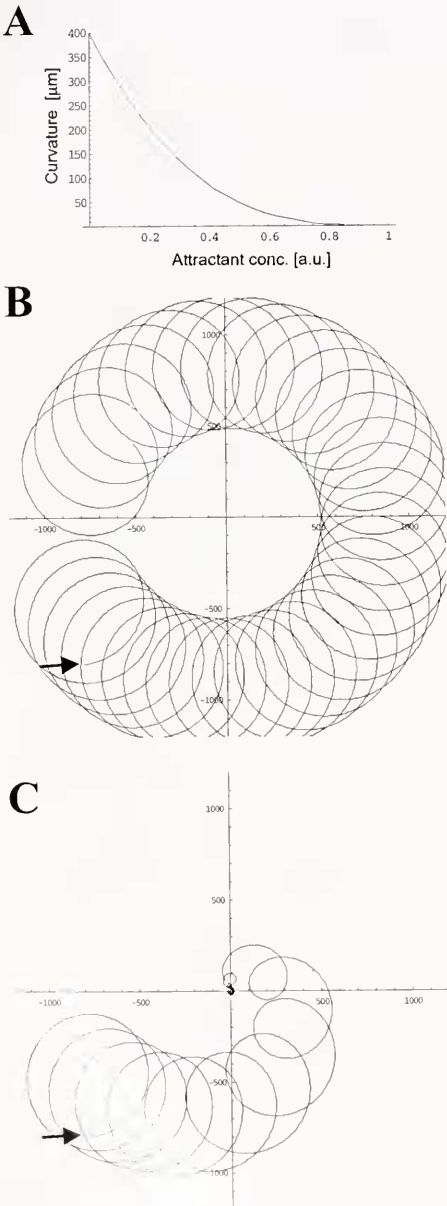
1000 μm) while they are far from the attractant source (~5 mm), and smaller trajectories (~200 μm) near the attractant source (~0.2 mm). However, this dependence on distance from the attractant was lost in the absence of external Ca^{2+}, which suggests that Ca^{2+} influx is involved in the modulation of the curvature of trajectories. We incorporated these findings into the assumptions set in the model as follows:

(a) Curvature decreases as intracellular Ca^{2+} concentration, ($[Ca^{2+}]_i$), increases (*i.e.*, a negative correlation).

(b) $[Ca^{2+}]_i$ positively correlates with $c(p)$, the attractant concentration which is sensed by the sperm.

Assumption (a) also agrees with the evidence that spermatozoa treated with a Ca^{2+} ionophore showed a curvature of ~200 μm, which increased up to ~800 μm at lower Ca^{2+} concentration. Since any quantitative relationship among these factors in real spermatozoa is not yet available, we set some trial functions and studied the behavior. We first tried a simple linear correlation between $[Ca^{2+}]_i$ and $c(p)$, and a cubic function for $[Ca^{2+}]_i$ and $r(t)$ (Fig. 3A):

$$[Ca^{2+}]_i = c(p) \quad (0 < c < 1; [\text{arbitral unit (a.u.)}]) \quad \text{(Eq. 6)}$$

$$r(t) = 400(1 - [Ca^{2+}]_i)^3 [\mu m] \quad (0 < [Ca^{2+}] < 1; [\text{a.u.}]) \quad \text{(Eq. 7)}$$

This now allows us to study how spermatozoa swim under these conditions. The results show that the trajectories generated by such conditions are far from chemotactic behavior. Spermatozoa do circle around the attractant source but never finally approach the egg (Fig. 3B). This result is not surprising because our present system is fully symmetric in terms of time and space components. When using functions other than those of equations (6 and 7), no chemotaxis is observed at all. However, a remarkable change occurs if we incorporate an additional condition:

(c) $[Ca^{2+}]_i$ has different rates of increase and decrease (slow to decrease).

This condition is not unlikely, because pumping of the cytosolic Ca^{2+} out of the cell or into the intracellular store against the electrochemical gradient across the membrane is an enzymatic process, which is energy-consuming, whereas Ca^{2+} influx generally occurs rapidly. Therefore, we then incorporated this additional condition as follows:

$$\Delta[Ca^{2+}]_i/\Delta t = -1/\tau([Ca^{2+}]_i - c(p))$$
$$\text{when} \quad [Ca^{2+}]_i > c(p) \quad \text{(Eq. 6')}$$

Figure 3. Simulations of the siphonophore model. (A) A cubic function as one of the examples of a function that negatively correlates attractant concentration to curvature of the trajectory. (B) A trajectory simulated with the function shown in (A). Time to lower $[Ca^{2+}]_i$ is not considered. The sperm started at position $(x, y) = (-800 \mu m, -800 \mu m)$ with an initial angle of 0.1 radian and a constant speed of 500 μm/s (arrow). The trajectory during the initial 40 s is shown. (C) A trajectory simulated under the same conditions as in (B), except that τ of 0.5 s is incorporated as a decay-time constant to lower $[Ca^{2+}]_i$.

A

Radius of curv. [μm]

ΔC/Δt [a.u./ms]

B

C

where τ is the decay time constant. This condition was applied only when $[Ca^{2+}]_i > c(p)$; otherwise, equation (6) was applied as before. When trajectories were calculated with these new sets of conditions (6, 6', 7), we found that the incorporation of a time component for the Ca^{2+} decay results in chemotactic trajectories (Fig. 3C) that are not unlike those obtained in the experimental observations. Likewise, chemotactic trajectories were reconstructed for a wide range of arbitrarily selected functions that relate '$c(p)$' to '$[Ca^{2+}]_i$,' positively instead of by equation (6), and relate '$[Ca^{2+}]_i$,' to '$r(t)$' negatively instead of by equation (7), even though some of them, of course, showed heavily distorted trajectories of approach toward the attractant source and unusually long or short times of approach.

The ascidian model

The behavior of ascidian sperm is quite different from that in the siphonophore sperm. The behavior illustrated in Figure 1B is based on observations of *Ciona intestinalis* by Ishikawa (2000) and Yoshida *et al.* (1993). In the presence of an attractant without a gradient, the curvature of the sperm trajectory is independent of the concentration of the attractant, and is close to that in the absence of the attractant (Fig. 1B). Under the gradient of attractant concentration, however, spermatozoa show rapid changes in their track diameters, so-called chemotactic turns. Since this turning behavior is lost in the calcium-free seawater (CFSW) or in the presence of Ca^{2+} channel inhibitors, it has been suggested that rapid changes of diameter are dependent on $[Ca^{2+}]_i$. Therefore, we again incorporated condition (a), as we did in the siphonophore model. Next, we need to infer the relationship between $[Ca^{2+}]_i$ and $c(p)$, the attractant concentration that the spermatozoan senses. Since modulation of diameter occurs only in the presence of an attractant gradient, we assumed that $[Ca^{2+}]_i$ depends on the temporal changes of $c(p)$ but not on the "absolute" concentration itself. Thus, we assume a second condition:

(d) $[Ca^{2+}]_i$ negatively correlates to the time derivative of the attractant concentration.

With conditions (a) and (d), it follows that $r(t)$ positively correlates to $\Delta c(p(t))/\Delta t$, the time derivative of the attract-

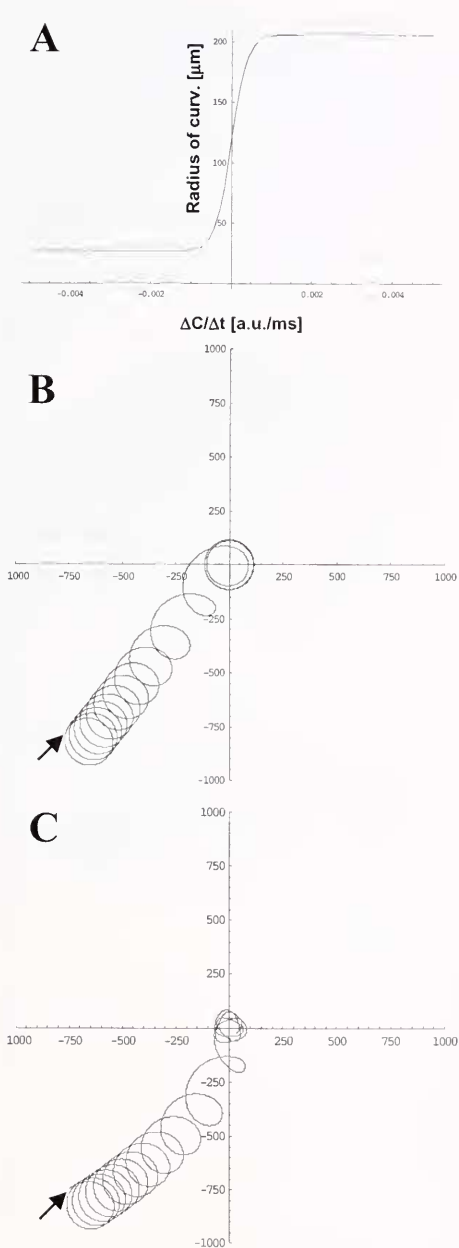**Figure 4.** Simulations of the ascidian model. (A) A sigmoid function as one of the examples of a function that positively correlates time-derived attractant concentration to the curvature of the trajectory. (B) A trajectory simulated with the function shown in (A). The sperm started at position $(x, y) = (-750\ \mu m, -750\ \mu m)$ with an initial angle of 0.8 radian and a constant speed of 250 $\mu m/s$ (arrow). The trajectory during the initial 40 s is shown. (C) A trajectory simulated under the same conditions as in (B), except that a delay of 150 ms in the response of curvature to the time-derived attractant concentration is incorporated.

ant concentration. This assumption was incorporated in the ascidian model as follows:

$$r(t) = F(\Delta c(p(t))/\Delta t) \qquad \text{(Eq. 8)}$$

Where F is the function that positively correlates $\delta c/\delta t$ with $r(t)$. We studied sperm behavior with a sigmoid function for F (Fig. 4A) and found that this condition alone is sufficient to show chemotactic trajectories with successive turns when approaching the attractant source (Fig. 4B). We further incorporated a delay in the sperm response of $r(t)$ to $\Delta c(p(t))/\Delta t$ with a time range of tens of milliseconds, because such a delay has been found in the analysis of the trajectory of real sperm (Ishikawa, 2000; Yoshida *et al.*, 2002). This resulted in similar trajectories, but with a twist (Fig. 4C), which is often observed in real chemotaxis in the ascidian. Thus, we find that the delay of sperm response is not an absolute necessity for chemotactic behavior in the case of the ascidian model, but this parameter results in trajectories that are somewhat more realistic.

Discussion

In the present study, we proposed two comprehensive models for strategies of sperm chemotaxis in the siphonophores and the ascidians. With these models, chemotactic trajectories similar to those observed for real spermatozoa could be reconstructed. We found that there are at least two ways to identify the location of the "hilltop"—the source of the chemoattractant—without looking around for it. The siphonophore's way is to "walk" circularly, with large-diameter curvatures at low altitude and smaller ones at higher altitude. This alone is not enough for success; however, success can be achieved if any increase in curvature is followed by a time lag. In the ascidian's way, one needs to sense the steepness (gradient) but not the height (absolute concentration): the curvature is large when climbing steeply uphill, medium when the slope is gentle, and small when

going downhill. The time-delay condition is not always necessary, but such a delay introduces twists into the trajectory.

Even though these models employ some conditions based on experimental results, these conditions may seem to be oversimplified. However, the goal of the present modeling study is not to simulate the natural behavior of the spermatozoa perfectly but to find out what elements are needed to reconstruct the phenomenon of interest. For this purpose, it is necessary to focus on a small number of important parameters.

Nonetheless, some lines of evidence in addition to those mentioned earlier, support our simplification of the conditions. First, it has been shown that asymmetrical bending waves are induced when a high concentration of Ca^{2+} is applied to the flagella of demembranated sea urchin sperm (Brokaw, 1979). This may support our condition (a). Next, it was recently suggested that a store-operated Ca^{2+} channel (SOC) regulates chemotaxis in the ascidian (Yoshida *et al.*, 2002). Involvement of such a SOC may account for the time delay in the curvature response to the temporal changes in the attractant concentration: this feature was often observed in the experiments and is introduced into the ascidian model (Fig. 4C), since activation of the SOC requires depletion of internal Ca^{2+} stores evoked by the releasing signals such as inositol 1,4,5-phosphate.

Quantitative comparison of the model outputs with experimental results is very important for validation of the models. Unfortunately, we are not ready to do such a study because the models currently have high degrees of freedom. The two functions, one that relates attractant stimulus with $[Ca^{2+}]_i$ and the other that relates $[Ca^{2+}]_i$ with curvature, cannot yet be quantitatively defined. Of course, one desirable experiment might be to experimentally define these functions and then to carry out a quantitative comparison. But this requires many very difficult technical break-
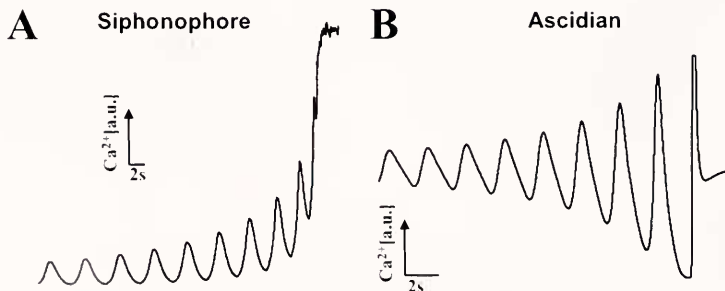

Figure 5. Changes in $[Ca^{2+}]_i$ during chemotaxis. (A) Plot of $[Ca^{2+}]_i$ as a function of time in the modeled chemotaxis for siphonophores (Fig. 3C). (B) Plot of $[Ca^{2+}]_i$ *versus* time in the modeled chemotaxis for the ascidian (Fig. 4B). It is assumed that $[Ca^{2+}]_i$ is proportional to the inverse of the radius of curvature.
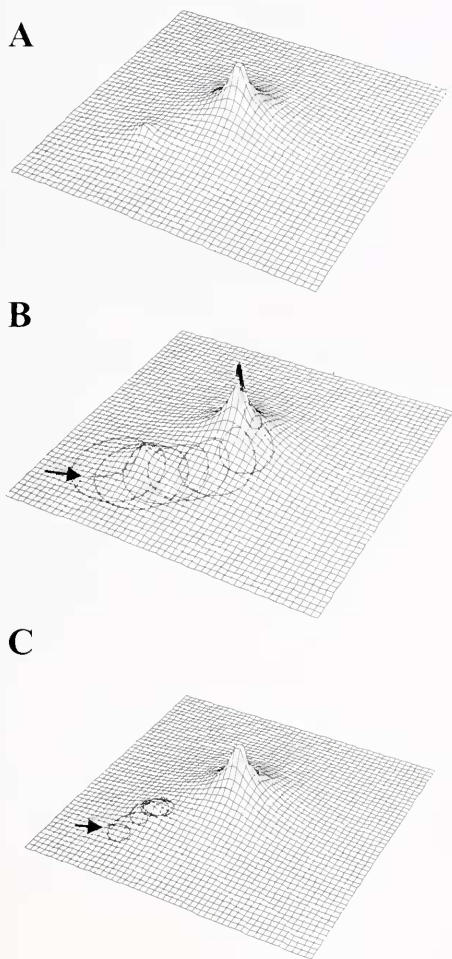
A

B

C

Figure 6. A difference in the sensitivity to a local attractant peak between the siphonophore and ascidian strategies. (A) A secondary source with one-fourth the attractant concentration of the main one is added at the position $(x, y) = (-500 \ \mu m, -500 \ \mu m)$. (B) Sperm trajectory with the siphonophore model under the dual peak profile in (A). The trajectory is superimposed upon the attractant profile. Note that the spermatozoa found the main peak. The initial condition is same as that in Fig. 3B. (C) Sperm trajectory simulated with the ascidian model. Note that the spermatozoa now found the local peak instead of the main peak. The initial condition is the same as that in Fig. 4B. Arrows in (B) and (C) indicate the initial positions and directions.

throughs such as quantification of local attractant concentration, application of an attractant stimulus varying with time, and so on. Another indirect but more practical exper-

iment would be to measure $[Ca^{2+}]_i$ during chemotaxis. Our models predict that there will be a temporal $[Ca^{2+}]_i$ pattern during chemotaxis specific to each model: $[Ca^{2+}]_i$ oscillates in both models, and the base level elevates in the siphonophores but not in the ascidians (Fig. 5). Even though measurement of $[Ca^{2+}]_i$ in swimming spermatozoa is still technically challenging, mainly due to the small volume of cytoplasm and fast movements of the sperm, we hope that recent innovations in Ca^{2+} indicators and image sensors will make it possible in the future.

What is the significance of the difference in the two strategies? Since temporal change of the attractant concentration is the critical parameter for the modulation of curvature in the ascidian model, we expect that the ascidian spermatozoon is more sensitive to local change of concentration than the siphonophore spermatozoon, in which the absolute concentration value is the most critical. Simulation under two attractant sources, one of high concentration and the other of low concentration, led to the expected results: the ascidian spermatozoa found the lower peak of attractant in the vicinity, and the siphonophore spermatozoa reached the higher peak (Fig. 6). Thus, an interesting future problem would be to test this prediction in biological experiments. One may also be interested in possible relationships between such characteristics of sperm strategy and the environment that the species are facing. However, such a question cannot be addressed currently. Most of our knowledge has been limited to sperm in two-dimensional laboratory conditions, even though the goal should be to reach a deep understanding of strategy in the three-dimensional natural environment. Since theoretical treatments suggests that drag forces near the interface have substantial effects on the flagellar motion of sperm (Katz, 1974), we should avoid applying knowledge gained in two dimensions thoughtlessly in building three-dimensional models. One needs to know how parameters that describe three-dimensional helical motions are affected by the attractant gradient. To accomplish this goal, we hope that techniques to measure sperm trajectories in the three-dimensional environment, as pioneered by Crenshaw *et al.* (2000), will soon be more accessible.

Acknowledgments

Literature Cited

Brokaw, C. J. 1979. Calcium-induced asymmetrical beating of Triton-demembranated sea urchin sperm flagella. *J. Cell Biol.* **82:** 401–411.

Coll, J. C., B. F. Bowden, G. V. Meehan, G. M. König, A. R. Carroll, D. M. Tapiolas, P. M. Alino, A. Heaton, R. De Nys, P. A. Leone, M. Maida, T. L. Acetet, R. H. Willis, R. C. Babcock, B. L. Willis, Z. Florian, M. N. Clayton, and R. L. Miller. 1994. Chemical aspects of mass spawning in corals. 1. Sperm-attractant molecules in the eggs of the scleractinian coral *Montipora digitata. Mar. Biol.* **118:** 177–182.

Cosson, M. P., D. Carré, and J. Cosson. 1984. Sperm chemotaxis in siphonophores. II. Calcium-dependent asymmetrical movement of spermatozoa induced by the attractant. *J. Cell Sci.* **68:** 163–181.

Cosson, J., P. Huitorel, and C. Gagnon. 2003. How spermatozoa come to be confined to surfaces. *Cell Motil. Cytoskelet.* **54:** 56–63.

Crenshaw, H. C., C. N. Ciampaglio, and M. McHenry. 2000. Analysis of the three-dimensional trajectories of organisms: estimates of velocity, curvature and torsion from positional information. *J. Exp. Biol.* **203:** 961–982.

Dan, J. C. 1950. Fertilization in the medusan *Spirocodon saltarix. Biol. Bull.* **99:** 412–415.

Eisenbach, M. 1999. Sperm chemotaxis. *Rev. Reprod.* **4:** 56–66.

Ishikawa, M. 2000. Strategy and regulation of sperm chemotactic behavior in the ascidian, *Ciona intestinalis.* M.S. thesis, University of Tokyo. (In Japanese).

Katz, D. F. 1974. On the propulsion of micro-organisms near solid boundaries. *J. Fluid Mech.* **64:** 33–49.

Kaupp, U. B., J. Solzin, E. Hildebrand, J. E. Brown, A. Helbig, V. Hagen, M. Beyermann, F. Pampaloni, and I. Weyand. 2003. The signal flow and motor response controlling chemotaxis of sea urchin sperm. *Nat. Cell Biol.* **5:** 109–117.

Miller, R. L. 1977. Distribution of sperm chemotaxis in the animal kingdom. Pp. 99–199 in *Advances in Invertebrate Reproduction,* Vol. 1. K. G. Adiyogi and R. G. Adiyogi, eds. Peralam Kenoth, Kerala, India.

Olson, J. H., X. Xiang, T. Ziegert, A. Kittelson, A. Rawls, A. L. Bieber, and D. E. Chandler. 2001. Allurin, a 21-kDa sperm chemoattractant from *Xenopus* egg jelly, is related to mammalian sperm-binding proteins. *Proc. Natl. Acad. Sci. USA* **98:** 11,205–11,210.

Ward, G. E., C. J. Brokaw, D. L. Garbers, and V. D. Vacquier. 1985. Chemotaxis of *Arbacia punctulata* spermatozoa to resact, a peptide from the egg jelly layer. *J. Cell Biol.* **101:** 2324–2329.

Yoshida, M., K. Inaba, and M. Morisawa. 1993. Sperm chemotaxis during the process of fertilization in the ascidians *Ciona savignyi* and *Ciona intestinalis. Dev. Biol.* **157:** 497–506.

Yoshida, M., M. Murata, K. Inaba, and M. Morisawa. 2002. A chemoattractant for ascidian spermatozoa is a sulfated steroid. *Proc. Natl. Acad. Sci. USA* **99:** 14,831–14,836.

Yoshida, M., M. Ishikawa, H. Izumi, R. De Santis, and M. Morisawa. 2003. Store-operated calcium channel regulates the chemotactic behavior of ascidian sperm. *Proc. Natl. Acad. Sci. USA* **100:** 149–154.